Available online at www.sciencedirect.com
ScienceDirect
Catalysis Today 119 (2007) 233–238
CATALYSIS TODAY
www.elsevier.com/locate/cattod

Effect of Mn/Al ratio in Co–Mn–Al mixed oxide catalysts prepared from hydrotalcite-like precursors on catalytic decomposition of N_2O

L. Obalová [a,*], K. Pacultová [a], J. Balabánová [b], K. Jirátová [b], Z. Bastl [c], M. Valášková [a], Z. Lacný [a], F. Kovanda [d]

[a] *Technical University of Ostrava, 17. listopadu 15, 708 33 Ostrava, Czech Republic*
[b] *Institute of Chemical Process Fundamentals ASCR, Rozvojová 135, 165 02 Prague, Czech Republic*
[c] *J. Heyrovsky Institute of Physical Chemistry ASCR, Dolejškova 3, 182 23 Prague, Czech Republic*
[d] *Institute of Chemical Technology, Technická 5, 166 28 Prague, Czech Republic*

Available online 8 September 2006

Abstract

The Co–Mn–Al mixed oxide catalysts were prepared by thermal decomposition of hydrotalcite-like precursors with Co/(Mn + Al) molar ratio of 2 and Mn/Al molar ratio varying from 0 to 2. The obtained catalysts were characterized by powder XRD, XPS, BET surface area and TPR measurements and tested in N_2O decomposition. The most active Co4MnAl catalyst exhibited both the optimum Mn/Al molar ratio and the optimum amount of components reducible in the temperature region in which the catalytic reaction proceeds (350–450 °C).

Keywords: N_2O decomposition; Mixed oxide catalysts; Hydrotalcite-like compounds

1. Introduction

Catalytic N_2O decomposition offers a simple solution of the control of N_2O in waste gases arising from combustion processes and chemical industry. However, sufficient catalyst activity is necessary for utilization of this simple method in practice [1,2]. Co-spinels prepared by calcination of Co-containing hydrotalcite-like compounds are thermally stable active catalyst for N_2O decomposition [3–10]. Recently we have studied the catalytic decomposition of N_2O over calcined Co–Mg–Mn–Al hydrotalcite-like compounds and we have found out that catalytic activity sharply increases after incorporation of Al into Co–Mn catalyst [11]. The aim of this contribution is a detailed study of the Al content effect on the activity of Co–Mn–Al mixed oxide catalysts in N_2O decomposition.

2. Experimental methods

The Co–Mn–Al hydrotalcite-like precursors were prepared by coprecipitation of nitrate solutions (the details were described previously in [11]). The catalysts were denoted according to the molar ratio of metal cation in the samples as Co4Mn2, Co4Mn1.5Al0.5, Co4Mn1.25Al0.75, Co4MnAl, Co4Mn0.75Al1.25, Co4Mn0.5Al1.5 and Co4Al2.

The powder XRD patterns were recorded using a Seifert XRD 3000P instrument, surface areas were determined by the BET method and the TPR measurements were carried out using hydrogen/nitrogen mixture up to 850 °C. Details are given in [11].

The XPS spectra were measured using ESCA 310 (Gamma-data Scienta, Sweden) photoelectron spectrometer. The measurements were performed using Al Kα radiation for electron excitation. The FWHM of Au $4f_{7/2}$ photoemission line of bulk Au standard was 0.65 eV. The samples were spread on a gold surface and spectra were recorded at room temperature and 6×10^{-8} Pa. The surface static charging of the samples was suppressed by using Scienta flood gun. The regions recorded were Co 2p, Co 3p, Mn 2p, Mg 1s, Al 2p, Al 2s, C 1s and O 1s. The spectra were

* Corresponding author. Tel.: +420 59 699 1532; fax: +420 59 732 3396.
E-mail address: lucie.obalova@vsb.cz (L. Obalová).

0920-5861/$ – see front matter
doi:10.1016/j.cattod.2006.08.027

curve-fitted after subtraction of Shirley background [12] using Gaussian-Lorentzian line shape. Quantification of the elemental concentrations was accomplished by correcting photoelectron peak intensities for their cross-sections [13].

The N_2O decomposition reaction was performed in fixed-bed reactor in the temperature range 330–450 °C with the total flow rate 50–100 ml/min NTP (273 K, 101,325 Pa), 0.1–0.3 g of sample with particle size 0.160–0.315 mm and 1000 ppm N_2O balanced by helium. The gas chromatograph with TCD was used to analyze N_2O.

3. Results and discussion

In the powder XRD patterns of all dried precursors except Co4Mn1.5Al0.5 and Co4Mn2 samples, only a well-crystallized hydrotalcite-like phase was detected (not shown here). An unidentified phase was found in the Co4Mn1.5Al0.5 and Co4Mn2 precursors. In the Co4Mn1.5Al0.5 sample it was an admixture beside hydrotalcite-like phase, while in the Co4Mn2 precursor it was the major component. Spinel-type mixed oxides were detected in the powder XRD patterns of the samples calcined at 500 °C. Comparison of the XRD patterns of the samples is given in Fig. 1. XRD characteristics of the presented catalytic system were described recently [14].

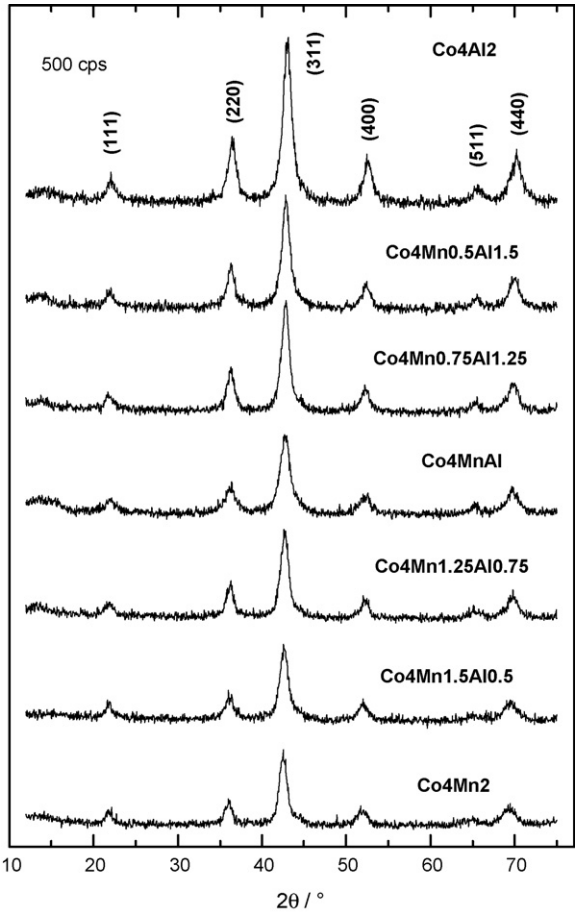

Fig. 1. Powder XRD diffraction patterns of hydrotalcite-like compounds calcined at 500 °C.

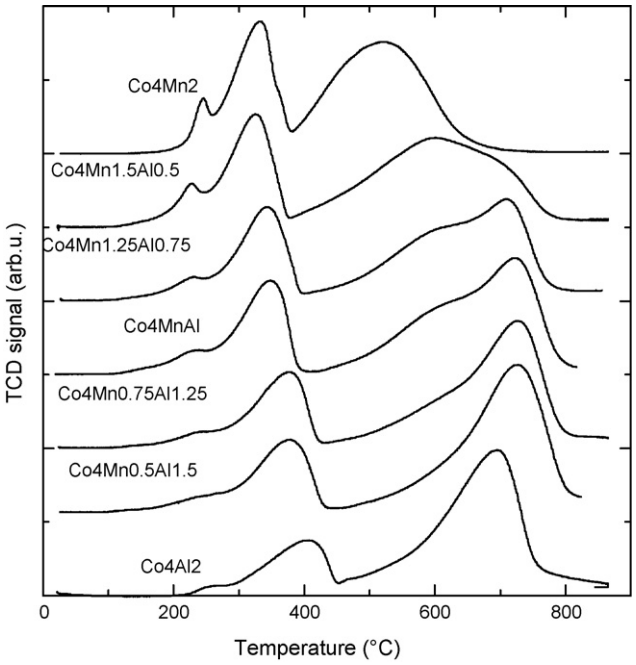

Fig. 2. Temperature-programmed reduction of the prepared catalysts.

The temperature-programmed reduction patterns of the prepared catalysts are shown in Fig. 2. TPR pattern of Co4Al2 showed two distinct reducible cobalt species. The species reducible around 400 °C are assigned to Co_3O_4, those reducible around 700 °C are ascribed to spinel-like phase as was described by Ribet et al. [15] previously. The low-temperature peak consists of two peaks. First part represents the reduction of Co^{3+} to Co^{2+} (250 °C) and the second part of this peak belongs to the reduction of Co^{2+} to Co^0 (400 °C) [16,17]. The reduction of cobalt in spinel-like phase proceeds in one step (700 °C). The consecutive substitution of aluminum in Co4Al2 catalyst for manganese caused: (i) gradual increase and the shift of the first part of the low-temperature peak, (ii) the shift of the second part of the low-temperature peak to lower temperature, and (iii) the shift of the high-temperature peak. The maximum of the high-temperature peak shifts to higher temperature at first and then decreases to lower temperature: Co4Al2 < Co4Mn0.5Al1.5 < Co4Mn0.75Al1.25 < Co4MnAl > Co4Mn1.25Al0.75 > Co4Mn1.5Al0.5 > Co4Mn2. The Co4Mn2 catalyst is reduced in two main temperature regions. The first one (200–400 °C) belongs to the reduction of Co^{3+} to Co^{2+} and to reduction of MnO_2, possibly Mn_3O_4–Mn_2O_3 or Mn_3O_4–MnO. The second peak (400–700 °C) of the Co-Mn mixed oxide represents deep reduction of Mn_2O_3 to MnO, as was established by TPR of standard Mn-oxide. Components reducible at the temperatures higher than the reaction temperature cannot likely contribute to the catalytic reaction. For that reason we determined the amount of components reducible in the reaction temperature region as that of hydrogen consumed in the range 350–450 °C (Table 3).

XPS data provide information about composition, obtained from core photoemission intensity data, and information about the chemical state of the elements in the near-surface region.

Table 1
Binding energies of core level electrons (±0.2 eV) and full widths at half maximum of the photoelectron peaks (in parentheses) of catalysts and standard materials

	Co $2p_{3/2}$		Co $2p_{3/2-1/2}$[a]	Co 3p	Mn $2p_{3/2}$		O 1s			Mn $2p_{3/2}$–O 1s[b]
Co4Al2	780.2 (1.9)	781.3 (2.2)	15.1	61.1 (3.1)	–		530.6	532.4 (1.8)		–
Co4Mn2	780.2 (1.9)	781.3 (2.2)	15.2	61.1 (3.2)	641.8 (2.1)	642.9 (1.9)	530.2	531.7 (1.2)	532.8	112.2
Co4MnAl	780.3 (1.9)	781.5 (2.2)	15.3	61.1 (3.1)	641.8 (2.1)	642.9 (1.9)	530.3	531.8 (1.3)	532.8	112.3
Co4Mn0.5Al1.5	780.3 (1.9)	781.5 (2.2)	15.2	61.1 (3.2)	641.7 (2.1)	642.9 (1.9)	530.3	531.7 (1.3)	532.7	112.4
Co4Mn1.5Al0.5	780.4 (1.9)	781.6 (2.2)	15.2	61.1 (3.2)	641.8 (2.1)	643.0 (1.9)	530.4	531.8 (1.3)	532.8	112.2
Co_3O_4	779.5 (1.2)	780.6 (2.3)	15.1	60.8 (2.9)	–		529.8	531.3 (1.0)	532.7	–
$CoC_{10}PF_6$		780.7 (1.4)	14.9	62.2 (2.7)	–		–			–
MnO	–		–	–	641.2 (2.4)		529.9	531.4 (1.3)	532.4	111.3
Mn_2O_3	–		–	–	641.5 (2.1)		529.9	531.3 (1.1)	532.2	111.6
MnO_2	–		–	–	642.3 (1.9)		529.9	531.3 (1.1)	532.2	111.4

[a] Co $2p_{3/2-1/2}$ effective spin-orbit splitting.
[b] O 1s (component with the lowest BE) to Mn $2p_{3/2}$ peak separation.

Binding energies (BE) of the selected photoemission lines of catalysts and standard materials are summarized in Table 1. As expected the binding energy of Mn 2p electrons for standard Mn oxides increases with increasing oxidation state of manganese. Other authors reported the same trends: Mn $2p_{3/2}$ BE 640.9, 641.8 and 642.5 eV for MnO, Mn_2O_3 and MnO_2 [18,19], 641.1, 641.4, 641.6 and 641.8 eV for MnO, Mn_2O_3, Mn_3O_4 and MnO_2, respectively [20,21]. Unequivocal determination of manganese chemical state in the measured samples only on the basis of comparison of the measured binding energy of Mn $2p_{3/2}$ electrons with binding energies obtained for oxide standards is rather difficult since Mn can be present in several different chemical states, the spectra of which are overlapping and close in energy. To identify the oxidation state, O 1s (the component with the lowest binding energy) to Mn $2p_{3/2}$ peak separation or 3s multiplet splitting are also useful [19,20]. There seems to be a clear evidence in the spectra of Mn 2p electrons that two chemical states, Mn^{3+} and Mn^{4+} with Mn^{3+} prevailing are present in catalysts (Table 2). This conclusion is based on comparison of the Mn $2p_{3/2}$ electron binding energies and values of Mn $2p_{3/2}$–O 1s peak separation in catalysts and in oxide standards MnO, Mn_2O_3 and MnO_2 (Table 2).

For identifying the cobalt chemical state the energy separation of $2p_{3/2}$ to $2p_{1/2}$ and satellite structure of Co 2p spectra are useful [22–24]. The presence of several components in catalyst samples was recognized from Co 2p electron spectra. They reveal the presence of both, Co^{2+} and Co^{3+} oxidation states. This conclusion is based on the two facts: (i) satellite lines are rather weak, (ii) the obtained value of the effective spin-orbit splitting 15.2 ± 0.1 eV corresponds well to the value typical for Co^{3+} and Co_3O_4 oxide with mixed valence of cobalt. The shift of binding energies of Co $2p_{3/2}$ electrons in catalysts towards higher values compared to Co_3O_4 could be related to the presence of other components (Al, Mn) in the samples.

Oxygen is present in several chemical states in all samples. The prevailing state is that with the lowest binding energy belonging to oxide form, while the spectra component with higher binding energy can be attributed to –OH, C=O and CO_3^{2-} groups [25] or to non-stoichiometric spinel like phase [3]. Oxygen with the highest binding energy could be assigned to C–OH, COO^- groups [25].

Comparison of both x(Co + Mn) values of bulk metal concentrations calculated from chemical analysis of the dried hydrotalcite precursors and surface metal concentrations of catalysts determined from XPS (Table 2) shows significant enrichment of the surface by Al and Mn. Similar enrichment of the surface by Al was observed recently in the calcined Co–Al [3], Cu–Mg–Al [26] and Ni–Al [27] hydrotalcites. Manganese enrichment occurred in $Mn_xCo_{1-x}O$ solid solutions (x = 0.2–0.4) at the expense of cobalt [28]. It follows from our results that the total concentration of Co and Mn cations on the surface (x(Co + Mn)) depends linearly on their bulk concentration (see inserted small figure in Fig. 4). The Mn^{3+}/Mn^{4+} ratio observed on the catalyst surface is roughly independent on the Mn amount in the catalyst sample, while the Co^{2+}/Co^{3+} ratio shows distinct maximum.

Table 2
Bulk metal concentrations calculated from chemical analysis of the dried hydrotalcite precursors and surface metal concentrations determined by XPS of the catalysts after thermal treatment at 500 °C

Catalytic system	Molar ratio Co/Mn		Molar ratio Co/Al		Molar ratio Mn/Al		Molar fraction x(Co + Mn)		Surface molar ratio	
	Bulk	Surface	Bulk	Surface	Bulk	Surface	Bulk	Surface	Co^{2+}/Co^{3+}	Mn^{3+}/Mn^{4+}
Co4Mn2	2.16	1.39	–	–	–	–	1.00	1.00	0.78	2.33
Co4Mn1.5Al0.5	2.70	1.54	7.38	2.86	2.73	1.86	0.91	0.835	1.32	2.42
Co4Mn1.25Al0.75	3.13	n.d.	5.08	n.d.	1.62	n.d.	0.87	n.d.	n.d.	n.d.
Co4MnAl	4.12	2.38	3.85	1.94	0.93	0.77	0.83	0.73	1.13	2.27
Co4Mn0.75Al1.25	5.34	n.d.	3.02	n.d.	0.56	n.d.	0.78	n.d.	n.d.	n.d.
Co4Mn0.5Al1.5	8.10	4.55	2.60	1.19	0.32	0.26	0.75	0.59	1.00	2.29
Co4Al2	–	–	1.92	0.92	–	–	0.66	0.48	0.92	–

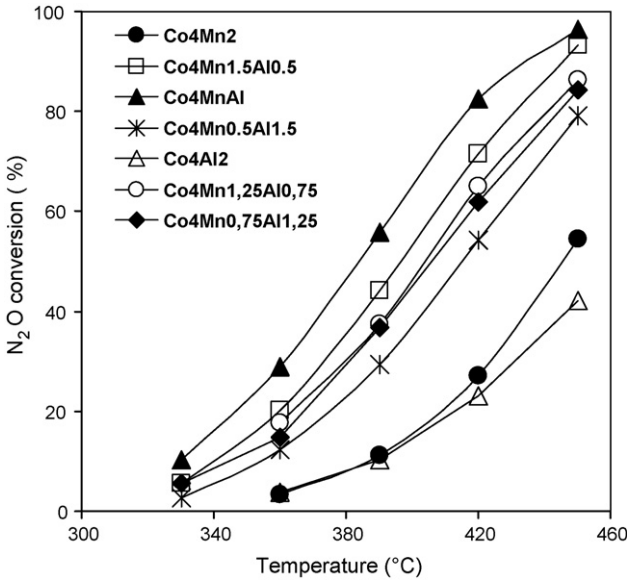

Fig. 3. Temperature dependence of N_2O conversion. Conditions: 1000 ppm N_2O balanced by He, overall flow: 100 ml/min, weight of catalyst: 0.1 g.

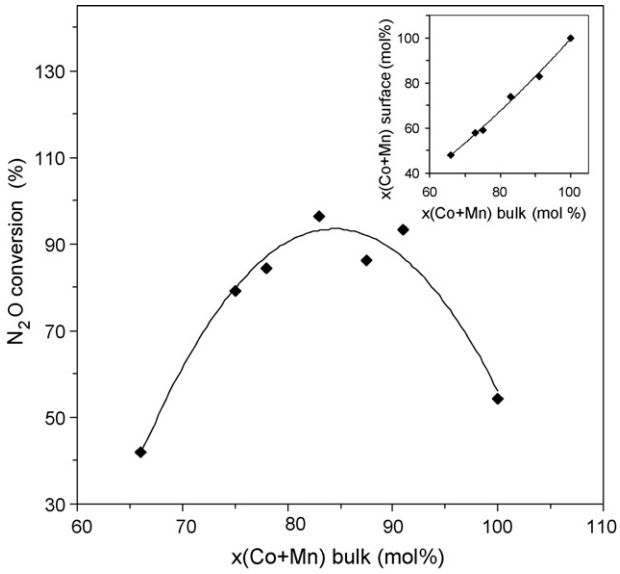

Fig. 4. Dependence of the N_2O conversion (450 °C, 0.1 g, 100 ml/min) on the bulk concentration of Co and Mn. Inserted figure: correlation between bulk and surface concentration of Co and Mn.

The temperature dependence of N_2O conversion is demonstrated in Fig. 3. Since the catalytic reaction proceeds on the catalyst surface area that differs for each sample, kinetic constants k^* [mol s^{-1} m^{-2} Pa^{-1}] were evaluated according to the first order rate law [3,29] (Table 3) to get the right evaluation of the effect of the chemical composition on the reaction rate. It was found out that these constants k^* decreased in order Co4MnAl > Co4Mn1.5Al0.5 > Co4Mn0.5Al1.5 ≥ Co4Mn0.75Al1.25 ≥ Co4Mn1.25Al0.75 > Co4Mn2 > Co4Al2. Although surface area is usually critical for determination of catalytic activity, a variation in specific surface area has been shown to have negligible effect because the activities order of k [mol s^{-1} g^{-1} Pa^{-1}] and k^* is almost the same.

Our previous results indicated that an optimum amount of components reducible in the temperature region 350–450 °C is necessary for achieving high catalytic activity in N_2O decomposition over Ni–(Mg)–Al–(Mn) and Co–(Mg)–Mn–Al calcined hydrotalcites [11,30]. The existence of such optimum can be explained by using the concept of polaron hopping mechanism [31] and is connected with oxidation–reduction mechanism of N_2O decomposition. As far as we accept the validity of this theory, an optimum surface concentration of Co and Mn should exist (Al is supposed to be inactive). Since we have found the surface concentration x(Co + Mn) is nearly linearly dependent on the bulk composition of (Co + Mn), an optimum value of bulk x(Co + Mn) corresponding to high catalytic activity can be expected and it was really found out in our work (Fig. 4).

The catalyst activity is dependent on metal–oxygen bond strength as implies from published mechanism of N_2O decomposition. The metal–oxygen bond strength is influenced by both valence and transition metal ion coordination. Weaker bond facilitates desorption of oxygen adsorbed on the surface after decomposition of N_2O molecule. The oxygen desorption is the rate controlling step during N_2O decomposition [1]. The N_2O decomposition was studied over low concentration of Mn^{3+} and Mn^{4+} dispersed in MgO [32]. The Mn^{3+} cations were much more active than Mn^{4+}. The most active manganese oxide was Mn_2O_3 compared to MnO, Mn_3O_4 and MnO_2 [33]. Octahedral coordinated Co^{2+} in $MgAl_2O_4$ was more active than tetrahedrally coordinated ion. Distortion of the structure resulting in two longer Co–O bonds and hence in weaker

Table 3
Some characteristics of the catalysts and kinetic constants of N_2O decomposition

Catalyst	S_{BET} (m^2/g)	TPR[a] (mmol H_2/g)	TPR[b] (mmol H_2/g)	k^c ($\times 10^9$ mol s^{-1} g^{-1} Pa^{-1})	k^{*c} ($\times 10^{11}$ mol s^{-1} m^{-2} Pa^{-1})
Co4Mn2	43.6	11.58	1.81	1.9	4.3
Co4Mn1.5Al0.5	89.9	11.92	0.84	9.7	10.8
Co4Mn1.25Al0.75	120.4	11.54	1.14	7.0	5.8
Co4MnAl	92.7	11.26	0.96	14.5	15.6
Co4Mn0.75Al1.25	115.8	10.86	1.66	7.4	6.4
Co4Mn0.5Al1.5	103.2	10.70	1.56	6.9	6.6
Co4Al2	82.1	9.55	0.66	1.8	2.2

[a] In the region 20–800 °C.
[b] In the region 350–450 °C
[c] Kinetic constants determined according to the first order rate law ($X_{N_2O} < 30\%$) at 420 °C.

bond strength [34] caused higher catalytic activity. It is supposed that two neighboring cations take part in the reaction over concentrated solid solutions. Thus the active center could be the M–O–M system formed of two transition metal ions differing in a charge and of oxygen situated between them. This type of active center was published for both manganese in $La_{1-x}Sr_xMnO_3$ perovskite [35] and cobalt in $NiCo_2O_4$ and in Co_3O_4 spinels [36]. The highest catalytic activity was achieved when molar ratios of the both components Mn^{3+}/Mn^{4+} and Co^{2+}/Co^{3+} were 1:1. This ratio made possible easier charge transfer from transition metal ion to the oxygen during N_2O chemisorption and back from O^- to transition metal ion during O_2 desorption. In our case we suppose that both Co and Mn contribute to the catalyst activity. So, highly active catalyst should contain both metals and they should occur on catalysts surface in optimum concentrations. In term of the Mn^{3+}/Mn^{4+} and Co^{2+}/Co^{3+} ratios, all our catalysts show slightly higher ratio of Mn^{3+}/Mn^{4+} than the optimum value mentioned above but almost optimum ratio of Co^{2+}/Co^{3+}. The catalyst activity could also be increased by optimization of cobalt and manganese distribution between tetrahedral and octahedral positions in the spinel structure.

4. Conclusions

The most active Co4MnAl catalyst contains both the optimum surface amount of cobalt and manganese and the optimum amount of components reducible in the temperature region 350–450 °C (the range in which the catalytic reaction proceeds) as is obvious from TPR measurements (Fig. 5).

The observed dependencies are in relation to the hypothetical mechanism of N_2O decomposition. With increasing amount of reducible components, the movement of electrons within the bulk and the surface become increasingly efficient and hence the N_2O adsorption process is facilitated. In case the amount of reducible components is higher than the optimum value, the ability of the catalyst to catalyze N_2O decomposition decreases. The reason for such finding could consist in a non-optimum geometric arrangement of the active sites on the catalyst surface and/or in a too strong oxygen bond to catalyst surface and consequently slow O_2 desorption.

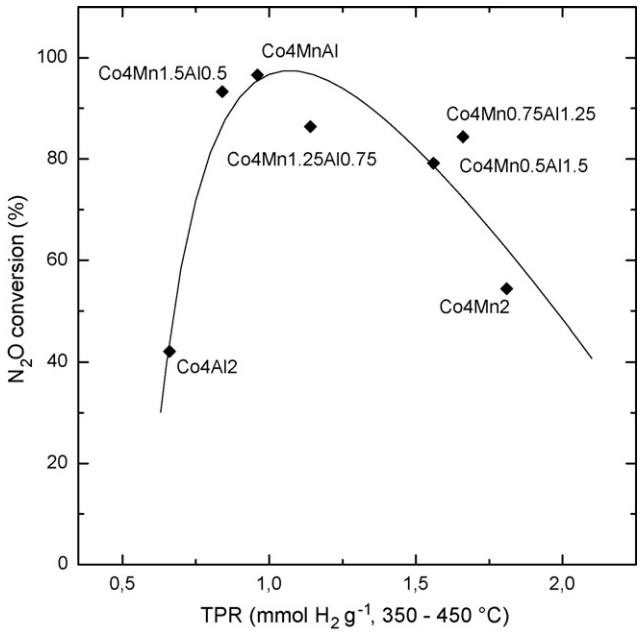

Fig. 5. Dependence of the N_2O conversion (450 °C, 0.1 g, 100 ml/min) on the amount of reducible components in the interval 350–450 °C.

Acknowledgements

This work was supported by the Grant Agency of the Czech Republic (grants no. 106/05/0366 and no. 104/04/2116) and by the Czech Ministry of Education, Youth and Sports (research projects CEZ: nos. 6046137302, 6198910016 and project no. 544/205/G1).

References

[1] F. Kapteijn, J.R. Mirasol, J.A. Moulijn, Appl. Catal. B 9 (1996) 25.
[2] J. Pérez-Ramírez, F. Kapteijn, K. Schöffel, J.A. Moulijn, Appl. Catal. B 44 (2003) 117.
[3] S. Kannan, C.S. Swamy, Catal. Today 53 (1999) 725.
[4] J.N. Armor, T.A. Braymer, T.S. Farris, Y. Li, F.P. Petrocelli, E.L. Weist, S. Kannan, C.S. Swamy, Appl. Catal. B 7 (1996) 397.
[5] C.S. Swamy, S. Kannan, Y. Li, J.N. Armor, T.A. Brayner, US Patent 5 407 652 (1995), to Engelhard Corporation.
[6] S. Kannan, Appl. Clay Sci. 13 (1998) 347.
[7] J. Pérez-Ramírez, F. Kaptejn, J.A. Moulijn, Catal. Lett. 60 (1999) 133.
[8] T.S. Farris, Z. Li, J.N. Armor, T.A. Braymer, US Patent 5 472 677 (1995), to Engelhard Corporation.
[9] J. Pérez-Ramírez, g. Mul, X. Xu, F. Kapteijn, J.A. Moulijn, in: A. Corma, F.V. Melo, S. Mendioroz, J.L.G. Fierro (Eds.), Studies in Surface Science and Catalysis, vol. 130, Elsevier Science, 2000, p. 1445.
[10] J. Pérez-Ramírez, F. Kapteijn, J.A. Moulijn, Appl. Catal. B 23 (1999) 59.
[11] L. Obalová, K. Jirátová, F. Kovanda, K. Pacultová, Z. Lacný, Z. Mikulová, Appl. Catal. B 60 (2005) 289.
[12] D.A. Shirley, Phys. Rev. B 5 (1972) 4709.
[13] J.H. Scofield, J. Electron Spectrosc. Relat. Phenom. 8 (1971) 128.
[14] F. Kovanda, T. Rojka, J. Dobešová, V. Machovič, P. Bezdička, L. Obalová, K. Jirátová, T. Grygar, J. Solid State Chem. 179 (2006) 812.
[15] S. Ribet, D. Tichit, B. Coq, B. Ducourant, F. Morato, J. Solid State Chem. 142 (1999) 382.
[16] B.A. Sexton, A.E. Hughes, T.W. Turney, J. Catal. 97 (1986) 390.
[17] Y. Lin, Y.-W. Chen, Mater. Chem. Phys. 85 (2004) 171.
[18] J.S. Ford, R.B. Jackman, G.C. Allen, Philosoph. Mag. A (1984) 657.
[19] M. Kantcheva, M.U. Kucukkal, S. Suzer, J. Mol. Struct. 482/483 (1999) 19.
[20] M. Chigane, M. Ishikawa, J. Electrochem. Soc. 147 (2000) 2246.
[21] J.F. Moulder, W.F. Stickle, P.E. Sobol, K.D. Bomben, in: J. Chastain (Ed.), Handbook of X-ray Photoelectron Spectroscopy, Perkin-Elmer Co., Eden Prairie, 1992, p. 227.
[22] H.A.E. Hagelin-Weaver, G.B. Hoflund, D.M. Minahan, G.N. Salaita, Appl. Surf. Sci. 235 (2004) 420.
[23] J.-G. Kim, D.L. Pugmire, D. Battaglia, M.A. Langell, Appl. Surf. Sci. 165 (2000) 70.
[24] D. Briggs, M.P. Seah, Practical Surface Analysis, Wiley, New York, 1990.
[25] J.-C.H. Dupin, D. Gonbeau, P. Vinatier, A. Levasseur, Phys. Chem. Chem. Phys. 2 (2002) 1319.
[26] S. Kannan, A. Dubey, H. Knozinger, J. Catal. 231 (2005) 381.
[27] F. Triffiro, A. Vaccari, O. Clause, Catal. Today 21 (1994) 185.
[28] M.A. Langell, F. Gevrey, M.W. Nydegger, Appl. Surf. Sci. 153 (2000) 114.
[29] K.S. Chang, H. Song, Z.-S. Park, J.-W. Woo, Appl. Catal. A 273 (2004) 223.

[30] L. Obalová, K. Jirátová, F. Kovanda, M. Valášková, J. Balabánová, K. Pacultová, J. Mol. Catal. A 248 (2006) 210.
[31] P. Pomonis, J.C. Vickerman, J. Catal. 55 (1978) 88.
[32] A. Cimino, V. Indovina, J. Catal. 17 (1970) 54.
[33] T. Yamashita, A. Vannice, J. Catal. 161 (1996) 254.
[34] C. Angeletti, F. Pepe, P. Porta, J. Chem. Soc. Faraday Trans. 1 (1978) 1595.
[35] S. Louis Raj, B. Viswanathan, V. Srinivasan, J. Catal. 75 (1982) 185.
[36] R. Sundararajan, V. Srinivasan, in: B. Viswanathan, C.N. Pillai (Eds.), Recent Developments in Catalysis, Technip, Paris, 1992, p. 381.